Nd-YAG Laser Beam and GTA Welding of Ti-6Al-4V Alloy

Abdel-Monem El-Batahgy, Tarasankar DebRoy

***Abstract*— Geometry, microstructure, mechanical and corrosion properties of the Nd-YAG laser welded Ti-6Al-4V alloy were studied and compared with those of the GTA butt welded joints. The results showed that the laser welding parameters played an important role in obtaining satisfactory joint quality. The extent of surface discoloration which is an indicator of atmospheric contamination was influenced mainly by flow rate of the shielding gas rather than its type or pre-weld cleaning technique. Laser square butt weld profile was significantly improved by shifting the focal point up to 2mm below the specimen surface. Autogeneous full penetration laser welded butt joints could be produced using a welding speed of up to 5m/min. In comparison with the GTA welding, the laser welding with its lower heat input resulted in a pronounced decrease in the distortion level as well as significant decrease in the fusion zone size. On the other hand, the laser welded specimens had higher hardness of the fusion zone. As a result, inferior impact and corrosion properties were expected. However, opposite results were obtained where the laser welded joint demonstrated better impact and corrosion properties. The results showed that the properties of the welded joints were influenced not only by the fusion zone microstructure but also by the fusion zone size.**

***Index Terms*— Ti-6Al-4V alloy, Nd-YAG laser welding, Fusion zone size, Mechanical properties, Corrosion resistance.**

I. INTRODUCTION

Since the introduction of titanium and its alloys in the early 1950s, they have been widely used in the aerospace, energy, and chemical industries. The combination of high strength to weight ratio, excellent corrosion resistance and mechanical properties makes titanium the best material for many important applications [1]-[3]. Today, titanium alloys are used for demanding applications such as the static and rotating gas turbine engine components. Some of the most critical civilian and military airframe parts are made of these alloys. The use of titanium has expanded to include applications in nuclear power plants, food processing plants, oil refinery heat exchangers, marine components and medical prostheses. Ti-6Al-4V is the most widely used titanium alloy and it accounts for about 70% of all Ti-alloys produced. It is a two phase α+β titanium alloy with aluminum as the alpha stabilizer and vanadium as the beta stabilizer. This high-strength alloy can be used at cryogenic temperatures and at high temperatures up to about 800°F (427°C). It is used in the aerospace, marine, power generation and offshore industries and as implant materials in the medical and dental fields [4]-[6]. Welding offers an efficient and cost-effective means of fabricating structural assemblies containing this alloy. Understanding how the mechanical and corrosion properties of the Ti-6Al-4V alloy joints are affected by the welding variables are important for their serviceability. Structures made of this titanium alloy are fabricated using mainly conventional fusion welding processes including gas tungsten arc (GTA) welding process [7]-[12]. However, titanium alloys are noted for being difficult to weld by conventional fusion welding.

Recently, new techniques have been considered to achieve reliable welds with minimum distortion for the fabrication of components of both conventional and non-conventional materials. Of these techniques, laser welding [13]-[15] that can provide a significant benefit for the welding of titanium alloys because of its precision and rapid processing capability. There is an increasing interest on the laser beam welding of Ti-6Al-4V alloy and good success has been reported [16]-[20]. However, little has been published about the weldability of this alloy using high power solid-state Nd:YAG laser [21]-[23]. Previous investigations have demonstrated that the rapid solidification and quench associated with laser welding affects the microstructure and properties of the welded joints [24]. In other words, the microstructure of both the weld metal and heat affected zone of Ti-6Al-4V alloy is affected by the cooling rate from the peak temperature as a function of heat input. Consequently, it is expected that the microstructure of fusion zone then, the mechanical and corrosion properties of welded joints are affected by type of the welding process. However, this research area is far from complete and more works are required for the successful selection of the efficient and cost-effective welding process for fabricating large structures of titanium alloys. The present study has been concerned with improved understanding of the weldability of Ti-6Al-4V alloy using a 4kW Nd-YAG laser beam in comparison with the conventional GTA welding process. The effect of laser beam welding process on size and microstructure of fusion zone then, on mechanical and corrosion properties of Ti-6Al-4V alloy was examined. The effects of pre-weld cleaning technique, shielding condition, welding speed and focused beam position on the joints quality were investigated. Moreover, the mechanical and corrosion properties of the laser beam welded joints were compared with those of the GTA welded joints.

Manuscript received November 03, 2014.
Abdel-Monem El-Batahgy, Central Metallurgical R&D Institute, Cairo, Egypt, +20 122 4608265
Tarasankar DebRoy, Pennsylvania State University, Pennsylvania, USA, +1 814 865 1974 .

II. EXPERIMENTAL PROCEDURE

The titanium alloy used in this study is a commercial Ti-6Al-4V (ASTM Grade 5) and its chemical composition is given in Table I. It is supplied in the annealed condition and its mechanical properties are given in Table II. Specimens with machined surfaces and dimensions of 150x100x4mm were prepared for autogenous bead-on-plate and square butt welds. Alignment and clamping of square butt joints were done accurately using precise fixture to prevent distortion. The laser system used is Nd-YAG laser with a maximum output power of 4kW in the continuous wave mode. Laser beam was focused to 0.45mm spot size using 100mm focal length lens and 4mm nozzle diameter. Laser power was calibrated using power meter before starting laser welding experiments. The laser welding parameters investigated include laser power (P), welding speed (S), defocusing distance (Dd) and shielding gas as shown in Table III. Welding speed was varied between 3 to 6m/min while defocusing distance was changed between -4 and +4mm. Weld pool shielding was done using 99.997% pure argon or helium gas at a flow rate of 10 to 30 l/min.

Table I Chemical composition of the used titanium alloy.

C	N	Fe	Al	V	O	H
0.01	0.01	0.17	6.1	3.9	0.06	0.001

Table II Mechanical properties of the used titanium alloy.

Tensile strength MPa	Yield strength MPa	Elongation %	Hardness HV	Impact absorbed energy J/mm^2
947	869	11	303	3.1

Table III Welding parameters.

Laser beam welding process

Weld joint	Power (kW)	Speed (m/min)	Defocusing distance (mm)	Shielding gas/ flow rate (l/min)
BOP	4	3 ~ 6	-4.0 ~ +4.0	Argon/ 10 ~ 30 Helium/ 10~30
Butt	4	4 ~ 6	0.0 ~ -2.0	Argon / 20

GTA welding process

Current (A)	Voltage (V)	Weld speed (m/min)	Shielding gas/ flow rate (l/min)
125	14	0.15	Argon/10

Weld surface preparation was done using two techniques. Some weld joints were chemically cleaned through an acetone wipe to remove dirt and grease from the machined edges, followed by etching in 3% HF-HNO_3 solution to remove the titanium oxide plus hydro-carbon embedded contaminants from the surface. Then, the surface was rinsed in distilled water and alcohol and dried using forced warm air. Other weld joints were mechanically cleaned using steel ball blasting technique followed by wiping in alcohol and drying using forced warm air. For comparison, single pass gas tungsten arc (GTA) butt weld was made using welding parameters indicated in Table III. For both laser and GTA welds, the weld pool was shielded using the same shielding gas and flow rate as trailing and backing shields.

All welded joints were subjected to different non-destructive and destructive tests based on section IX of the ASME Code. Cross sections of welded joints found to be acceptable based on visual and radiographic tests were prepared for metallographic examinations using standard techniques. The shape and size of fusion zone was investigated using low magnification stereoscope while the microstructure was examined using optical microscopy. The Vickers hardness profiles were measured for polished and etched specimens at mid-thickness across the weld zone, HAZ and base metal applying a load of 500g for a dwell time of 25s. Face and root sides bend test was conducted using 10t bend radius to check ductility of welded joints. Transverse tensile test was performed at room temperature with a constant crosshead displacement rate of 3mm/min using Shimadzu 1000kN universal testing machine. The tensile test specimens have 50mm gage length, 4mm thickness, 12.5mm width (in the gage length region) and overall length of 200mm. Charpy Impact, fracture toughness, test was carried out at 0^{o}C (32^{o}F) on machined specimens taken from predetermined locations in weld metal and HAZ of both laser beam and GTA welded joints using Roell Amsler 300J testing machine. Standard test specimen could not be prepared due to low thickness of the plates. Then, subsize specimen with 55x10x2.5mm dimensions according to EN ISO 148-1 was prepared. For both tensile and impact tests, three test samples in the as-welded condition were tested for each welding process. In addition, the base metal was also tested. The average values of each property were determined. Accelerated corrosion test of laser beam and GTA welded specimens was carried out at 37^{o}C (98.8^{o}F) using Tafel polarization where potential-current curves were recorded to estimate corrosion rates. For this purpose, specimens were exposed to 3.5% sodium chloride under open-circuit condition for 30 minutes until E-corr became constant. Then, current is passed through the specimen for another 30 minutes to measure the relation between potential and current, from which the corrosion rates were deduced.

III. RESULTS AND DISCUSSION

3.1. Laser Bead-on-Plate Welds

3.1.1. Effect of pre-weld cleaning technique and shielding gas type and flow rate

Solid-state cracking and porosity are often encountered in Ti-alloy welds. However, these defects can be readily avoided by cleaning of the work piece and shielding of the weld zone from atmospheric contamination. Commonly cleaning is done using chemical methods [25]. In the current study, cleaning was done using both chemical and mechanical techniques. It is found that the cleaning technique had no significant effect on the weld quality. Both visual and radiographic examinations of laser welds made using either chemical or mechanical cleaning technique resulted in no unacceptable external or internal welding defects. Photographs of the laser beam welds made using 4kW laser power, 4m/min welding speed, 0.0mm defocusing distance and 20 l/min flow rate of different shielding gases are shown in Fig. 1. Visual examination indicated different degrees of surface

discoloration that in turn gave a good indication of the degree of atmospheric contamination. Argon shielding has resulted in a non-uniform weld appearance or irregularities in weld colour including light and dark straw colours as well as light blue, which indicated light or acceptable atmospheric contamination (Fig. 1-a). Such surface contamination/oxide was easily removed using stainless steel wire brush. As shielding gas was replaced with helium, the weld colour became uniform and changed to a bright silvery metallic luster in appearance indicating better shielding condition (Fig. 1-b). Discolouration at the outer edges of the HAZ is not generally significant and may be ignored. In other words, helium shielding is more efficient to avoid atmospheric contamination in comparison with argon shielding under same flow rate of 20 l/min. However, radiographic examination of laser welds made using either argon or helium shielding disclosed soundness of the welds and no unacceptable internal welding defects were observed. However, either lower or higher flow of shielding gas resulted in undesirable atmospheric contamination. Excess flow of shielding gas resulted in a loss of shielding as a result of turbulence.

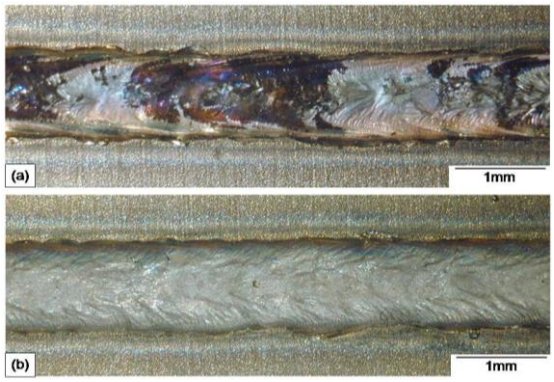

Fig. 1 Photographs of face side of laser beam welded joints made using 4kW, 4m/min, 0.0mm, and 20 l/min of different shielding gases. (a) argon shield, (b) helium shield.

3.1.2 Effect of welding speed

The welding speed affects the quality of the welded joints more than the laser power since it significantly influences both size and shape of the welds [26]. Therefore, the laser power was kept constant at the maximum available level of 4kW. The effect of welding speed was investigated using bead-on-pate welds. Macrographs of cross sections of laser beam welds made using 4kW laser power, 0.0mm defocusing distance, 20 l/min argon flow rate and different welding speeds are shown in Fig. 2. In all cases, the fusion zone was symmetrical about the axis of the laser beam. Full penetration was obtained when the welding speed was lower than 6m/min (Fig. 2-a, b). Increasing the welding speed resulted in a considerable reduction in the cross-sectional area of the fusion zone as a result of increasing its penetration depth/width ratio that means better quality. The weld zone depth/width ratio as a function of welding speed is shown in Fig. 3.

The fusion zone depth/width ratio was increased sharply from 1.7 to 4.1 when the welding speed was increased from 3 to 5m/min. However, the ratio decreased slightly with further increase in the welding speed owing to the reduction of heat input. In other words, the depth/width ratio was decreased with reducing the welding speed due to increasing the heat input leading to unacceptable weld profile. It can be deduced that 5m/min is considered as the optimum welding speed since it resulted in full penetration with minimum fusion zone size and better weld profile due to low heat input. With this high welding speed, attenuation of beam energy by plasma is less significant. This in turn results in relatively more exposure of the laser beam on the specimen surface. Consequently, weld depth/width ratio would be increased and the fusion zone size would be minimized that in turn results in minimizing distortion and residual stresses in addition to much better weld appearance. Such optimized high welding speed is considered as one of the most notable features of laser welding process concerning not only quality but also productivity. Studies by other researchers indicated that maximum welding speed for full penetration of 4mm thick Ti-6Al-4V plate using 7.7kW CW-CO2 laser was 3m/min while in the case of 4kW CW Nd: YAG laser, it was 1.2m/min [27].

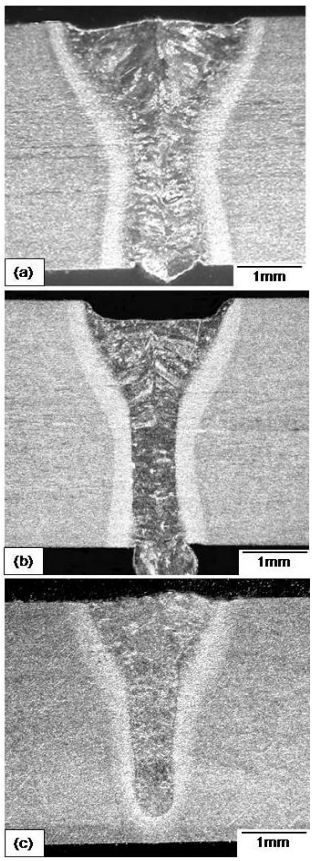

Fig. 2 Photographs of cross sections of laser beam welds made using 4kW, 0.0mm, 20 l/min Ar and different welding speeds. (a) 4m/min, (b) 5m/min, (c) 6m/min.

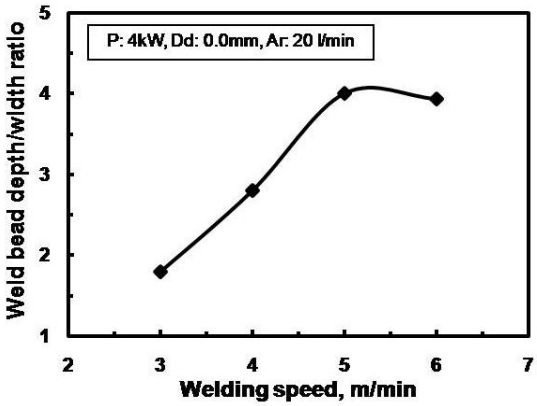

Fig. 3 Laser weld bead depth/width ratio as a function of welding speed.

3.1.3. Effect of defocusing distance

Defocusing distance, focus position, is the distance between specimen surface and the optical focal point. In order to clarify its effect on both penetration depth and weld profile, bead-on-plate welds were made. In this regard, higher welding speed (5.5m/min) than the optimum one (5m/min) was used to obtain incomplete penetration. Examples of laser weld cross sections made using 4kW laser power, 5.5m/min welding speed, 20l/min argon flow rate and two different defocusing distances are shown in Fig. 4. In comparison with focusing the laser beam at the specimen surface (Fig. 4-a), shifting the focused beam 2mm below the specimen surface (Fig. 4-b) has resulted in decreasing the penetration depth due to the decrease in laser beam density at the surface. However, a better weld configuration having a smooth curved fusion zone and better face appearance was obtained with shifting the focused beam 2mm below the specimen surface. In addition, results of radiographic examination confirmed absence of internal microporosities in this case as a result of stability of the laser welding process as well as more efficient shielding due to decrease in the standoff distance.

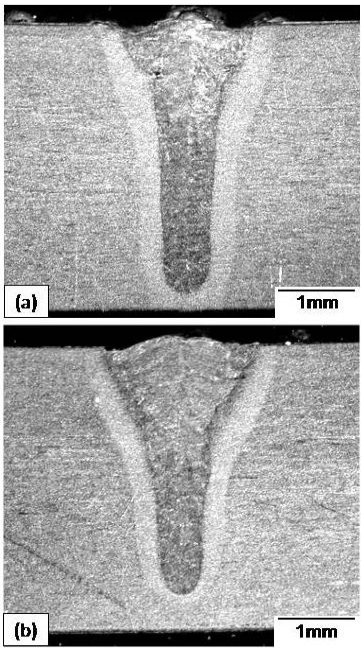

Fig. 4 Examples of laser weld cross sections made using 4kW, 5.5m/min, 20 l/min Ar and two different defocusing distances. (a) Dd: 0.0mm, (b) Dd: -2mm.

The influence of defocusing distance on the weld penetration depth has been confirmed using different welding parameters as shown in Fig. 5. The maximum penetration depth was obtained with focusing the laser beam at the specimen surface. The penetration depth was decreased from 3.9mm to either 3.8 or 3.7mm with shifting the focused beam 1mm either below or above the specimen surface. Further shift of the focused beam either below or above the specimen surface resulted in a remarkable decrease in the penetration depth, particularly with shifting the focused beam above the specimen surface. This is related mainly to sharp decrease in the laser beam density at the specimen surface. It was observed that porosity was formed in this case due to inaccurate standoff distance that means insufficient shielding condition. These results indicated that the most effective range of focused beam position to get maximum penetration is very narrow and lies between the specimen surface and 0.5mm below the surface. However, shifting the focused beam up to 2mm below the specimen surface has resulted in better weld profile as well as better quality where porosity and spatter were avoided due to better process stability.

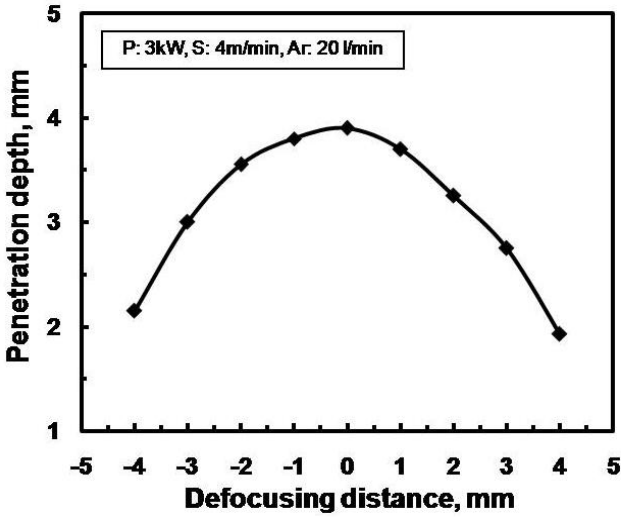

Fig. 5 Laser weld penetration depth as a function of defocusing distance.

3.2. Macrostructure of Laser and GTA Butt Welded Joints

The above results have shown that the optimum laser welding parameters to obtain acceptable weld profile are 4kW laser power, 5m/min welding speed, -2mm defocusing distance and 20 l/min argon for the 4mm thick plates. For a laser square butt weld joint, keeping a constant gap close to zero is of remarkable importance for a better weld profile. However, this is practically difficult particularly, for large size components that in turn results in unacceptable weld profile due to under-filling. Then, the focused beam was shifted 2mm below the specimen surface to reduce the effect of gap variation and to help in stabilizing the welding process. Argon was used as a shielding gas since it is more readily available and less costly. The pre-weld cleaning was done using chemical method.

Macrograph of a cross section of laser square butt welded joint made using the optimum laser welding parameters is shown in Fig. 6-a while that of GTA welded joint made using 125A, 14V, 0.15m/min, 10 l/min Ar is shown in Fig. 6-b. Visual and radiographic examinations of both laser and GTA welded joints showed full penetration and no unacceptable external or internal welding defects were observed. This may be partly due to proper selection of welding conditions implemented in both cases and confirms good reproducibility of the processing parameters selected. Besides, laser beam welding has resulted in a remarkable decrease in distortion level as indication of lower welding residual stresses due to low heat input. Macroscopic examination confirmed the soundness and full penetration of both laser and GTA welded joints. However, fusion zone profile and penetration depth/width ratio were significantly affected by the welding process. Typical laser weld profile with almost parallel surfaces and a slight taper configuration was obtained (Fig. 6-a). For GTA welded joint, it can be deduced that the development of the weld pool was essentially symmetrical about the axis of the electrode.

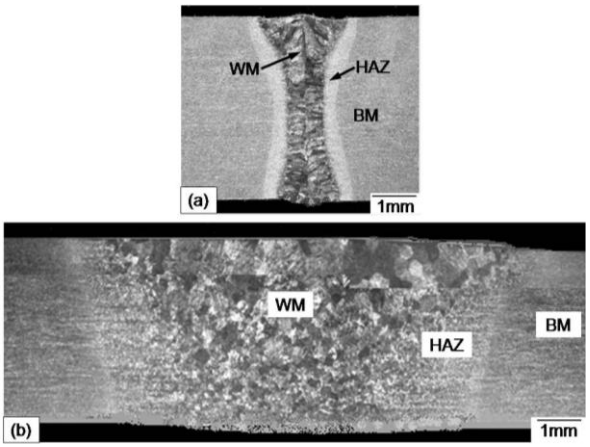

Fig. 6 Macrographs of cross sections of (a) laser butt welded joint produced using 4kW, 5m/min, -2mm, 20 l/min Ar and (b) GTA butt welded joint produced using 125A, 14V, 0.15m/min, 10 l/min Ar.

In comparison with GTA welding, laser beam welding process resulted in a remarkable decrease in cross-sectional area of the fusion zone to less than quarter as well as a sharp increase in the depth/width ratio to more than four times. The obtained depth/width ratio of GTA welded joint is relatively lower than the values reported in the literature. This discrepancy may be explained by the fact that the welds considered here are stationary welds. Under these conditions, the weld pool temperature is higher, resulting in a negative $d\gamma/dT$ over a large area causing a predominantly outward flow. This in turn would transport heat from the center to the periphery of the weld, which can explain the low depth/width ratio.

3. 3. Microstructure of Laser and GTA Butt Welded Joints

Optical micrographs with different magnifications of the Ti-6Al-4V base plates are shown in Fig. 7. The structure is typical of annealed alpha-beta alloy. It shows a mixture of fine alpha and beta phases where an equiaxed alpha titanium and intergranular beta phase are observed. Equiaxed alpha structures are formed by working in the alpha-beta range and then annealing at lower temperatures. An average hardness value of 303HV was obtained for this microstructure. Optical micrographs of a cross section of laser butt welded joint produced using the optimum laser welding parameters are shown in Fig. 8. The notable feature of weld metal is the highly directional nature of its microstructure around the axis of the laser beam as a result of high solidification rate. The microstructure of weld metal consists of large-grain transformed beta structure containing mainly fine acicular alpha-prime martensite (Fig. 8-b). It can be deduced that coarse columnar prior beta grains have been developed in weld metal upon solidification and this microstructure is completely different from that of the base metal. The high cooling rate associated with the laser welding process has promoted the transformation of beta to a fine acicular alpha-prime martensite, which exhibits high strength and hardness but low ductility and toughness. Regarding HAZ adjacent to fusion line, its microstructure is almost similar to that of the base metal which consists of a mixture of fine primary equiaxed alpha grains outlined by intergranular beta (Fig. 8-c). Besides, its width is confined only to less than 100μm (Fig. 8-a) as a result of the low heat input.

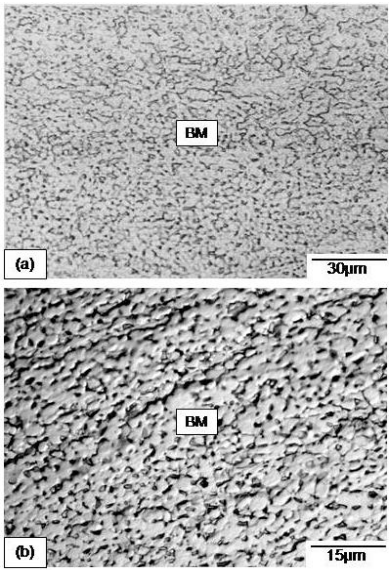

Fig. 7 Optical micrograph of the used Ti-6Al-4V base metal.

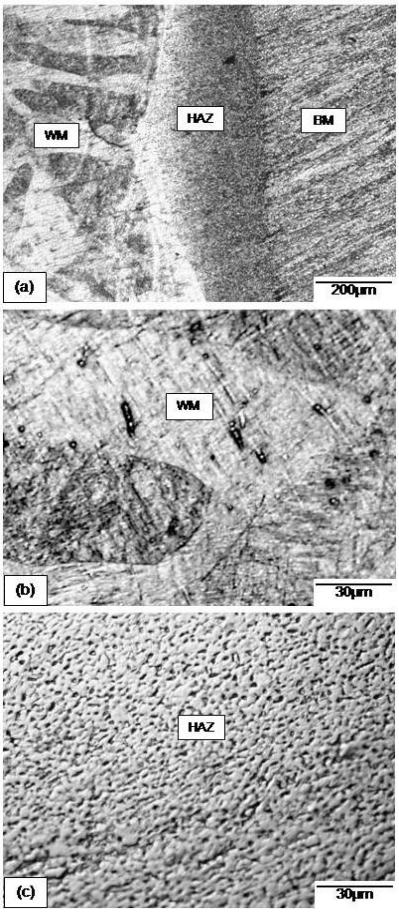

Fig. 8 Optical micrographs of a cross section of laser butt welded joint produced using optimum parameters. (a) fusion boundary, (b) weld metal, (c) HAZ adjacent to fusion line.

Optical micrographs of a cross section of the GTA butt welded joint are shown in Fig. 9. The weld metal microstructure has no directional nature around the weld center as a result of slow solidification rate. Higher magnification of the GTA weld metal disclosed that its microstructure consists mainly of coarse acicular structure

(Fig. 9-b) as a result of slow cooling. This microstructure exhibits better ductility and toughness combined with acceptable strength level. In comparison with the laser welded joint, a wider HAZ width was obtained (Fig. 9-a). HAZ microstructure adjacent to fusion line is coarser than that of the laser welded joint where it is a mixture of primary alpha and transformed beta containing acicular alpha (Fig. 9-c). Variation in the microstructure among different welds can be rationalized based on the heating and cooling cycle of Ti-6Al-4V alloy. The structure of this alloy is completely beta at completion of solidification. On cooling in the solid state, transformation of beta to alpha occurs at temperatures below the alpha solves. The type of microstructure formed in both weld metal and HAZ is dependent on the cooling rate as a function of the heat input. For GTA welding, the transformation from beta to alpha occurs under slow cooling rate as a result of high heat input and the resultant microstructure contains less amount of alpha prime martensite. Concerning laser welding, the high cooling rate due to the low heat input will result in mainly fine acicular alpha-prime martensite. When the fusion zone of Ti-6Al-4V alloy is fully martensitic after fast cooling, they are more susceptible to cracking. In practice, weld cracking does not appear to be a serious problem with Ti-6Al-4V alloy, but has been reported by some investigators [28], [29]. Such cracking was not observed in the current investigation.

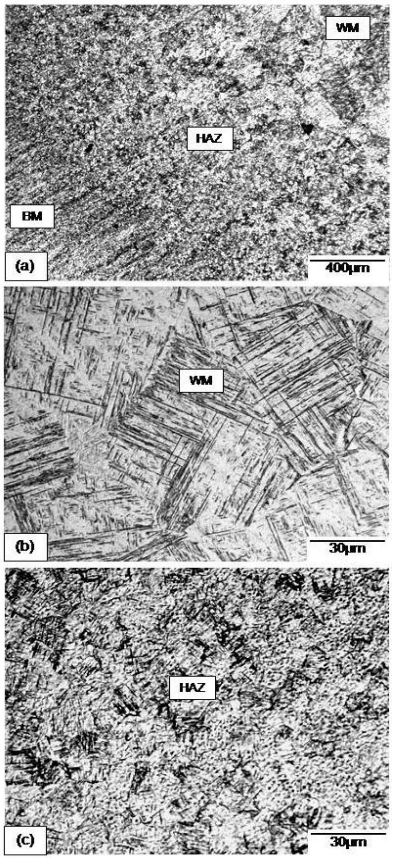

Fig. 9 Optical micrographs of a cross section of GTA butt welded joint. (a) fusion boundary, (b) weld metal, (c) HAZ adjacent to fusion line.

Typical hardness profiles in the weld metal, HAZ and base metal of the laser and GTA welded joints are shown in Fig. 10. The width of both weld metal and HAZ of the laser beam welded joint is considerably narrower than that of the GTA welded joint. Regardless of the welding process type, it is clear that the highest hardness values were obtained in the weld zone and the hardness gradually decreased from the weld center to the base metal due to the local differences of microstructure. However, the hardness values of weld metal and HAZ of the laser beam welded joint are significantly higher than those of the GTA welded joint. This is attributed to the higher amount of acicular alpha-prime as a result of higher cooling rate during laser welding.

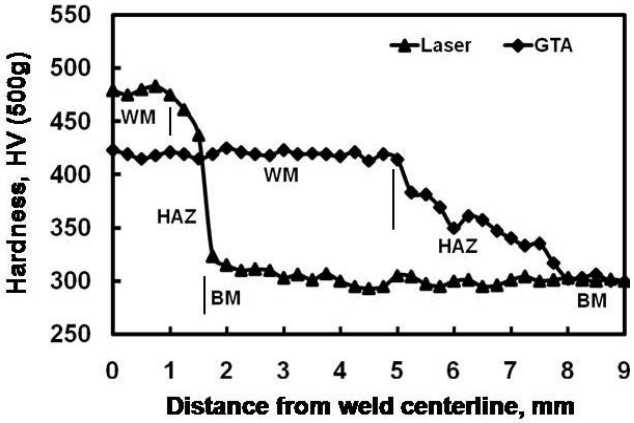

Fig. 10 Hardness profiles of weld metal, HAZ and base metal of the laser beam and GTA welded joints.

3.4. Mechanical Properties

The results of both face and root bend test showed sufficient degree of soundness and good ductility particularly, for the laser beam welded joints where no cracks were found after 10t bend radius was made. For tensile test, the laser beam welded specimens failed in the base metal, away from both weld and HAZ. On the other hand, the tensile fracture of the GTA welded specimens occurred in the weld zone. In comparison with the GTA welded specimens, higher ductility was confirmed for the laser welded specimens. Figure 11 shows the tensile strength of laser and GTA welded joints together with that of the base metal. It is observed that the tensile strength of the welded joints is influenced by the welding process. In comparison with the GTA welded joint, higher tensile strength was obtained for the laser welded joint. Tensile strength of the laser welded joint (943MPa) is almost 100% of that of the unaffected base metal (947MPa) while lower tensile strength was obtained for the GTA welded joint (899MPa). This is attributed to the formation of higher amount of acicular structure of the of laser welded joint.

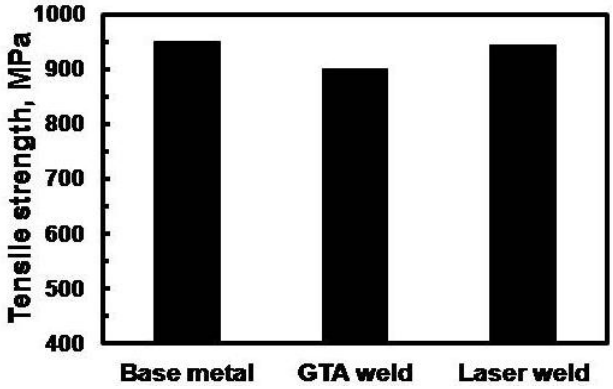

Fig. 11 Comparison of tensile strength of the laser beam and GTA welded joints with that of the base metal.

However, it is believed that the microstructure of the fusion zone is not the only controlling factor in maintaining the tensile properties of a welded joint and the effect of fusion zone size should also be considered. In other words, the tensile properties of welded joint are influenced not only by the microstructure of fusion zone but also by the fusion zone size for the two welding processes. The significant reduction in the fusion zone size of laser welded joint could also be important for maintaining its tensile strength. This could be related to lower welding residual stresses as indicated by a lower distortion level due to a lower heat input. The tensile strength level of laser welded joint is in agreement with ASME Code, which specify that the minimum tensile strength of butt welded joint should be equal to that of the base metal.

The GTA welded joint exhibited lower tensile strength and lower hardness than those of the laser welded joint. Therefore, the GTA weld was expected to have better fracture toughness. However, the impact energy of the GTA welded joint was lower than those of the laser welded joint. The impact energy of the laser welded joint was close to that of the base metal as shown in Fig. 12. This confirms that the impact fracture toughness of the welded joints is influenced not only by the weld zone microstructure but also by the fusion zone size. It shows that both the fusion zone size and the fusion zone microstructure affect the impact properties. In other words, the good impact fracture toughness of the laser welded Ti-6Al-4V alloy is supported by the small fusion zone size of the laser welded joint. It is expected that the impact fracture toughness will be influenced by variation of microstructure of fusion zones only when the fusion zone sizes are similar.

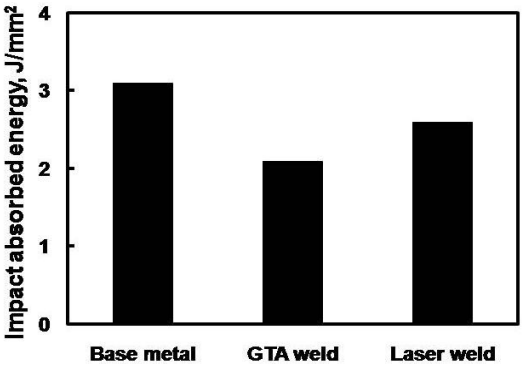

Fig. 12 Comparison of impact absorbed energy of the laser beam and GTA welded joints with that of the base metal.

3.5. Pitting Corrosion

The accelerated corrosion test of the laser and GTA welded joints was carried out using specimens containing similar size of the fusion zone surrounded by the base metal. Polarization curves and corrosion rate of laser and GTA welded specimens are shown in Figs. 13 and 14, respectively. The results of corrosion tests showed that corrosion behavior of the laser welded joint was better than that of the GTA welded joint. This behavior is observed in spite of the higher alpha-prime martensite content in the laser weld, which is expected to negatively impact corrosion resistance. The result indicates that the corrosion resistance of welded joint is influenced not only by the microstructure but also by the fusion zone size. Because the corrosion of the base metal was negligible, the weight loss is limited by the volume of the fusion zone available for corrosion. This means that the corrosion rate is influenced by the fusion zone size. The laser welded joint with its much smaller fusion zone size did not have the pronounced weight loss observed for the GTA welded joint. The fusion zone size had a pronounced effect on corrosion resistance compared to the effect of microstructure. In other words, the remarkable reduction in fusion zone size of the laser welded joint is more important for the higher corrosion resistance than the effect of microstructure. It can be deduced that the corrosion resistance of welded joints will be influenced mainly by microstructure of the fusion zone only when the fusion zone sizes are roughly equal.

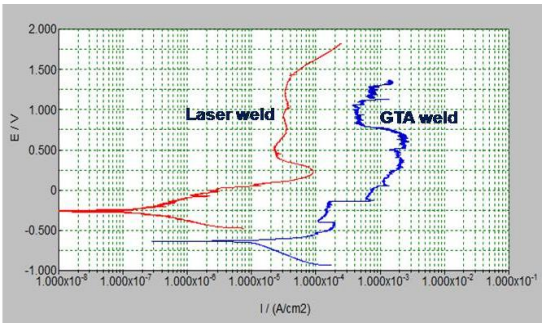

Fig. 13 Polarization curves of laser beam and GTA welded specimens.

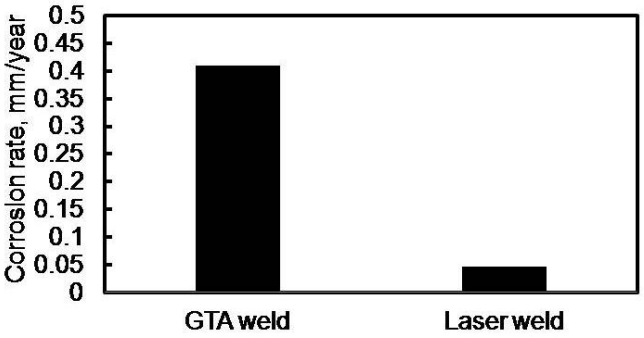

Fig. 14 Corrosion rate of laser beam and GTA welded joints.

IV. CONCLUSIONS

Based on the results achieved in this study, the following conclusions can be drawn.

Pre-weld surface cleaning by chemical or mechanical means had no notable difference on the weld quality. Use of argon or helium shielding gases had no significant effect on the degree of atmospheric contamination and either of the gases can be used for producing acceptable welds. However, flow rate of the shielding gas should be optimized since excess gas flow resulted in a loss of shielding due to turbulence.

The maximum penetration depth was obtained by focusing the laser beam at the specimen surface. However, shifting the focused beam up to 2mm below the surface resulted in better weld profile and improved process stability as evidenced by lower porosity and spatter. Full penetration with high quality of laser autogeneous square butt welded joint of 4mm thick Ti-6Al-4V alloy sheet was successfully produced using 5m/min welding speed with the maximum available 4kW Nd:YAG laser power. Such high laser welding speed is of considerable importance not only for good weld quality but also for high production rate.

Laser welded specimens showed much lower distortion and smaller fusion zone size than the GTA welded specimens. On the other hand, the laser welded samples had higher hardness in the fusion zone due to higher amount of acicular alpha prime martensite which resulted from the higher cooling rate. However, the laser beam welded samples with their harder microstructure exhibited better impact and corrosion properties. This means that properties of the welded joints were influenced not only by the microstructure but also by the fusion zone size for the two welding processes. The significant reduction of laser fusion zone size was more important for maintaining tensile, impact and corrosion properties, compared to the effect of microstructure.

ACKNOWLEDGEMENT

This research was supported by NSF Award ID: OISE-0711136, US-Egypt Cooperative Research on Modeling of Welding of Titanium Alloys.

REFERENCES

[1] G. Welsch, R. Boyer and E. W. Collings (eds.): Materials Properties Handbook-Titanium Alloys, ASM International, Materials Park, Ohio, USA, 1994, pp. 73-98.
[2] L. Christoph and P. Manfred, editors: Titanium and Titanium Alloys-Fundamentals and Application, Wiley-VCH Verlag GmbH & Co., Weinheim, Germany, 2003, pp. 27-65.
[3] R. R. Boyer: An overview on the use of titanium in the aerospace industry, Mater. Sci. Eng. A, 213, 1-2, 1996, pp. 103-114.
[4] G. Lütjering: Influence of processing on microstructure and mechanical properties of (α+β) titanium alloys, Mater. Sci. Eng.: A, 243, 1-2, 1998, pp. 32-45.
[5] J. Tiley, T. Searles, E. Lee, S. Kar, R. Banerjee, J. C. Russ and H. L. Fraser: Quantification of microstructural features in α/β titanium alloys, Mater. Sci. Eng.: A, 372, 1-2, 2004, pp. 191-198.
[6] M. Niinomi: Mechanical properties of biomedical titanium alloys, Mater. Sci. Eng.: A, 243, 1-2, 1998, pp. 231-236.
[7] A. B. Short: Gas tungsten arc welding of α + β titanium alloys: a review, Mater. Sci. Tech., 25, 3, 2009, pp. 309-324.
[8] V. P. Prilutsky and S. V. Akhonin: TIG welding of titanium alloys using fluxes, Weld. in the World, 58, 2, 2014, pp. 245-251.
[9] Z. Sun and D. Pan: Welding of titanium alloys with activating flux, Sci. Tech. Weld. Join., 9, 4, 2004, pp. 337-344.
[10] M. Balasubramanian, V. Jayabalan and V. Balasubramanian: Effect of pulsed current gas tungsten arc welding parameters on microstructure of titanium alloy welds, J. Manuf. Sci. Eng., 131, 6, 2009, 4 pages doi:10.1115/1.4000373
[11] M. Balasubramanian, V. Jayabalan and V. Balasubramanian: Effect of microstructure on impact toughness of pulsed current GTA welded α–β titanium alloy, Mater. Lett., 62, 2008, pp. 1102-1106.
[12] S. Sundaresan, G. D. Janaki Ram and G. Madhusudhan Reddy: Microstructural refinement of weld fusion zones in α–β titanium alloys using pulsed current welding, Mater. Sci. Eng.: A, 262, 1-2, 1999, pp. 88-100.
[13] M. P. Graham, D. M. Hirak, H. W. Kerr and D. C. Weckman: Nd-YAG laser welding of coated sheet steel, J. Laser Appl., 6, 1994, pp. 212-222.
[14] A. Matsunawa, A. El-Batahgy, and B. Zaghloul: Laser beam welding of lap joints of dissimilar materials, Trans. of JWRI, 2, 1998, pp. 36-44.
[15] A. El-Batahgy: Effect of laser beam welding parameters on fusion zone shape and microstructure of austenitic stainless steel, Mater. Lett., 32, 2-3, 1997, pp. 155-163.
[16] E. Akman, A. Demir, T. Canel and T. Sınmazçelik: Laser welding of Ti6Al4V titanium alloys, J. Mater. Proc. Tech., 209, 8, 2009, pp. 3705-3713.
[17] F. Caiazzo, V. Alfieri, G. Corrado, F. Cardaropoli and V. Sergi: Investigation and optimization of laser welding of Ti-6Al-4V titanium alloy plates, J. Manuf. Sci. Eng., 135, 6, 2013, 8 pages doi: 10.1115/1.4025578.
[18] X Zhao, J Zhang, X Song and W Guo: Investigation on mechanical properties of laser welded joints for Ti–6Al–4V titanium alloy, Mater. Sci. Tech., 29, 12, 2013, pp. 1405-1413.
[19] S-H. Wang, M-D. Wei and L-W. Tsay: Tensile properties of LBW welds in Ti–6Al–4V alloy at evaluated temperatures below 450°C, Mater. Lett., 57, 2003, pp. 1815-1823.
[20] Y. Zhao, J. Huang, Y. Zhao and Y-X Wu: Microstructure and mechanical properties of laser welded lap joints of Ti-6Al-4V Alloy, Adv. Mater. Res., 311-313, 2011, pp. 2375-2378.
[21] T. Patt, F. Rumenap and W. Viol: Nd-YAG laser beam welding of the titanium alloy Ti-6Al-4V, Europeon Conference on Laser Treatment of Materials, Sept. 22-23 1998, Hanover, Germany
[22] X. Cao and M. Jahazi: Effect of welding speed on butt joint quality of Ti-6Al-4V alloy welded using a high-power Nd:YAG laser, Opt. Lasers Eng., 47, 2009, pp. 1231-1241.
[23] E. Akman, T. Canel, A. Demir and T. Sinmazcelik: Optimization of pulsed Nd-YAG laser parameters for titanium seam-welding, AIP Conf. Proc. 899, 2007, pp. 303-304.
[24] R. R. Boyer and R. R. Wallem: The effect of cooling rate on the properties of beta annealed Ti-6Al-4V, Microstructure/property relationships of titanium alloys, S. Ankem and J. A. Hall, eds., TMS, Warrendale, PA, 1994, pp. 125-132.
[25] N.N. Prokhorov: Hot cracking resistance of Ti-alloys in welding, Weld. Prod., 33, 9, 1986, pp. 40-42.
[26] A. El-Batahgy, A. Khourshid and T. Sharef: Effect of laser beam welding parameters on microstructure and properties of duplex stainless steel, Mater. Sci. Appl., 2, 4, 2011, pp. 1443-1451.
[27] F. Coste, P. Aubry, H. Launais, and R. Fabbro: Optimizing the quality of TA6V and inconel laser welding on airplane part manufacturing, Proceedings of International Congress ICALEO, 1999, pp. 261-269.
[28] H. Inoue and T. Ogawa: Weld cracking and solidification behavior of titanium alloys, Weld. J., 69, 7, 1990, pp. 131-137.
[29] J. L. Huang, N. Warnken, J-C. Gebelin, M. Strangwood and R. C. Reed: On the mechanism of porosity formation during welding of titanium alloys, Acta Mater., 60, 6-7, 2012, pp. 3215-3225